Carbohydrate Polymers 343 (2024) 122455

Contents lists available at ScienceDirect

Carbohydrate Polymers

journal homepage: www.elsevier.com/locate/carbpol

In situ formed aldehyde-modified hyaluronic acid hydrogel with polyelectrolyte complexes of aldehyde-modified chondroitin sulfate and gelatin: An approach for minocycline delivery

Tutut Habibah [a,b], Jana Matonohová [a], Jaromír Kulhánek [a], Una Fitzgerald [c], Marek Ingr [b], Martin Pravda [a,*], Abhay Pandit [c], Vladimír Velebný [a]

[a] Contipro a.s. Dolní Dobrouč 401, Dolní Dobrouč, 56102, Czechia
[b] Faculty of Technology, Tomas Bata University in Zlin, Vavrečkova, 5669, Czechia
[c] CURAM, SFI Centre for Research on Biomedical Devices, Biomedical Engineering, University of Galway, Upper Newcastle, H91 W2TY, Ireland

ARTICLE INFO

Keywords:
Hydrogel
Minocycline
Hyaluronic acid
Chondroitin sulphate
Polyelectrolyte complexes

ABSTRACT

Polysaccharides like hyaluronan (HA) and chondroitin sulfate (CS) are native of the brain's extracellular matrix crucial for myelination and brain maturation. Despite extensive research on HA and CS as drug delivery systems (DDS), their high water solubility limits their application as drug carriers. This study introduces an injectable DDS using aldehyde-modified hyaluronic acid (HAOX) hydrogel containing polyelectrolyte complexes (PEC) formed with calcium, gelatin, and either CS or aldehyde-modified CS (CSOX) to deliver minocycline for Multiple Sclerosis therapy. PECs with CSOX enable covalent crosslinking to HAOX, creating immobilized PECs (HAOX_PECOX), while those with CS remain unbound (HAOX_PECS). The in situ forming DDS can be administered via a 20 G needle, with rapid gelation preventing premature leakage. The system integrates into an implanted device for minocycline release through either Fickian or anomalous diffusion, depending on PEC immobilization. HAOX_PECOX reduced burst release by 88 %, with a duration of 127 h for 50 % release. The DDS exhibited an elastic modulus of 3800 Pa and a low swelling ratio (0–1 %), enabling precise control of minocycline release kinetics. Released minocycline reduced IL-6 secretion in the Whole Blood Monocytes Activation Test, suggesting that DDS formation may not alter the biological activity of the loaded drug.

1. Introduction

Multiple sclerosis (MS) is a brain degenerative disease characterized by focal lesions due to inflammatory demyelination in the central nervous system (CNS) (Mahad et al., 2015). MS gives rise to brain mass loss (Andravizou et al., 2019) leading to symptoms like speech difficulties, loss of motor skills, and cognitive impairment (Wajda & Sosnoff, 2015). In 2020, there were almost 1,200,000 cases of MS in Europe (EMSP, 2021) and over 22,000 MS-related deaths worldwide (Lugaresi et al., 2023). Despite years of research, the underlying cause of MS remains unclear. Treatment options are limited by complex decision-making due to the multi-faceted symptoms (Wajda & Sosnoff, 2015). Individuals diagnosed with multiple sclerosis are prescribed Disease-Modifying Therapies (DMT) to slow down the disease progression and decrease the frequency of relapses. These drugs are administered through various methods, including oral, injections, and infusion therapy (Gajofatto & Benedetti, 2015). Recent innovations in medical technology have facilitated the ease of DMT administration in patients by introducing electromechanical autoinjectors (Barone et al., 2016; Y. T. Lin et al., 2023) and oromucosal spray devices (Creta et al., 2022). These innovations allow individuals to self-administer their treatments, thus minimizing the need for frequent visits to healthcare professionals. While these devices offer flexibility and convenience in terms of application, timing, and location, they still require the active participation of the patients. For instance, an autoinjector for DMT may require refilling every other day, whereas spray applicators must be refilled daily (Russo et al., 2015). Unfortunately, patients' non-compliance or negligence can lead to adverse effects and suboptimal dosing.

To minimize the frequency of drug administration and to improve the user-friendliness of these devices, a current study explores patients' preferences for implanted drug delivery reservoirs. The reservoirs aim to reduce the active involvement of patients in the treatment process

* Corresponding author.
E-mail address: Martin.pravda@contipro.com (M. Pravda).

https://doi.org/10.1016/j.carbpol.2024.122455
Received 15 March 2024; Received in revised form 28 June 2024; Accepted 1 July 2024
Available online 2 July 2024

(Visser et al., 2021). The primary challenge of this endeavor is developing a controlled release system that can be integrated into these devices. The design of such a device requires a system capable of retaining a high concentration of DMT and releasing it in a timely manner without significantly alternating in its structure (Tan et al., 2022). The distinct physical properties of hydrogels have attracted considerable attention in their application for drug delivery. Their porous structures can be finely adjusted by regulating the cross-link density. This permeable nature facilitates the entrapment of DMT into the gel matrix and subsequent controlled drug release, contingent upon the diffusion coefficient of the specific small molecule or macromolecule through the gel network (Li & Mooney, 2016a).

Hyaluronic acid (HA) hydrogel with tunable mechanical and physicochemical properties can produce a low to non-swelling hydrogel, conserving the original mechanical properties and size stability, which is suitable for this purpose. A previous study on low-swelling HA hydrogel demonstrated that these systems can effectively control the release of bioactive molecules for up to three weeks (Toropitsyn, Ščigalková, Pravda, Toropitsyna, & Velebný, 2023; Toropitsyn, Ščigalková, Pravda, & Velebný, 2023). Furthermore, the delivery system offered injectability and mechanical properties, achievable by varying polymer concentrations and cross-linking density. Notably, the release mechanism is mainly governed by Fickian diffusion, eliminating the need for active patient interventions (Toropitsyn, Ščigalková, Pravda, & Velebný, 2023). Further research has introduced a double network (DN) structure comprising rigid and elastic polymer networks. The highly crosslinked rigid network dissipates applied stress on the hydrogel in this DN structure. In contrast, the less cross-linked flexible network, embedded within the rigid one, provides support, maintaining the shape of the DN hydrogels (Huang et al., 2021).

The interpenetration of the two networks leads to a rise in the cross-linking between polymer chains, which in turn decrease the porosity of the hydrogels and minimizes swelling (Gong et al., 2003). A study of DN hydrogel confined in a cassette prepared from hyaluronan and chondroitin sulphate demonstrated a low equilibrium swelling ratio of 1.7 after 80 days while maintaining its structural integrity. The observed swelling profile also indicates the contribution of physical confinement, which prevents the gel from swelling in response to water absorption, which later enhances the long-term stability (Mihajlovic et al., 2022). Furthermore, this DN structure mimics the composition of brain tissue, which is rich in HA and CS (Lwata & Carlson, 1993; Singh & Bachhawat, 1968). However, the high-water solubility of HA and CS limits their application as drug carriers. The suitability of aldehyde-modified derivatives of hyaluronic acid and chondroitin sulphate for biomedical applications was demonstrated to be nontoxic materials. The presence of reactive aldehyde groups in these materials makes them ideal for reacting with aminooxy compounds via the Oxime Click reaction, which results in the formation of hydrogel in situ. This reaction is both rapid and orthogonal to functionalities found in biomolecules and cells, with water being the by-product and no catalyst required (Bobula et al., 2016; Buffa et al., 2015).

Studies on hydrogel-based drug delivery for CNS diseases have shown that Minocycline can be effectively entrapped within a hydrogel structure to regulate its release profile (Ghosh et al., 2019; Wang et al., 2017). The lipophilicity of minocycline allows it to cross the blood-brain-barrier and reach its target sites (Asadi et al., 2020). Minocycline has anti-inflammatory and neuroprotective properties independent of its antimicrobial function (Garrido-Mesa et al., 2013). It has been found to reduce disease activity and inflammation in the CNS while regulating immunological responses in the periphery. Studies have shown that minocycline can deactivate microglia and reduce the production of pro-inflammatory cytokines, such as interleukin-1 β (IL-1β) and interleukin-6 (IL-6) (Henry et al., 2008), which can inhibit T-cell activation. However, the therapeutic effects of minocycline depend on its dosage and stability profile (Elewa et al., 2006). While frequent dosing can compensate for a low level of minocycline in the brain, chronic administration can result in multiple side effects (Metz et al., 2017). Further research studies are required to develop innovative drug delivery systems to enhance the efficacy of minocycline.

Studies on minocycline -controlled release have highlighted the combination of hydrogel and polyelectrolyte complexes (PEC) of sulphate-bearing polymers, calcium chloride (CA), and gelatin to address the issue of rapid release (Holmkvist et al., 2016; Wu et al., 2018; Zhang et al., 2014). Minocycline can chelate divalent metal ions, such as calcium ions. When organic molecules contain sulphate or sulfonate functionalities, minocycline /Ca^{2+} interacts with the negatively charged sulphate or sulfonate, forming complexes with reduced water solubility (Soliman et al., 2010). Moreover, the immobilization of minocycline within the PEC and stabilization of the PEC structure were enhanced by positively charged gelatin type A (GA) (Zhang et al., 2014). This opposite charge interaction creates reversible structures such as nanoparticles (Holmkvist et al., 2016), micelles (Soliman et al., 2010) or films that can shield minocycline from degradation and extend its release profile for up to 30 days (Zhang et al., 2014). Combining PEC-loaded hydrogels allows minocycline to be protected from environmental factors and integrated into specific locations.

Herein we report the development of a novel injectable hydrogel containing a PEC of minocycline and biopolymers. The hydrogel is formed in situ after injecting the precursor solution into an application site, such as a reservoir or tissue. Two variations of hydrogels containing unbound and immobilized PEC, were prepared separately (Fig. 1). The hypotheses for this study are as follows. First, the release profile of minocycline from the DDS is expected to vary based on the immobilization state of the PEC, with immobilized PEC hindering the release more effectively than unbound PEC. Second, the incorporation of PEC is anticipated not to affect the cross-linking process, resulting in uniform gelation times across different formulations and enabling tunable viscoelastic properties for optimal injectability. Third, the preparation method of the DDS was expected to preserve the bioactivity of minocycline. Besides introducing a new PEC immobilization method, current DDS allows straightforward entrapment strategy for minocycline, avoiding drug-polymer conjugation and ensuring the release of the drug in its active form. Furthermore, it utilizes hyaluronic acid's hydrogel with minimal swelling to enable precise drug release and simplified the clinical use through the improved in situ injectability. This hydrogel delivery platform was designed to provide a controlled and gradual drug release into the environment. DDS are highly customizable and adaptable to different biological parameters of interest, making them a promising tool for CNS drug delivery applications.

2. Materials and methods

The materials used in this study were aldehyde-modified HA (HAOX 25, Mw 325 kDa, DS 7.1 %) provided by Contipro a.s. (Czechia), Minocycline (M9511, CAS: 13614–98-7) from Sigma-Aldrich (Czechia), injection syringes and needles from Servoprax GmbH (Wesel, Germany), a Human IL-6 Enzyme-linked immunosorbent assay (ELISA) Kit from Invitrogen (Czechia), Endotoxin standard (BRP, E0150000) from Merck (Czechia), Pig skin gelatin (140 bloom, Art.Nr. 4275.3) from Carl ROTH GmBH (Karlsruhe, Germany), Sodium chloride (NaCl, Cat No.:16610) and Calcium Chloride Hexahydrate ($CaCl_2.6H_2O$, CAS: 7774-34-7) from Lach-ner (Czechia), and Bovine Chondroitin Sulphate (CS, 10–40 KDa, Prod. Code: F0511) with an isomer ratio of chondroitin sulphate A (C4S) to chondroitin sulphate C (C6S) is 4/6 obtained from Bioiberica (Spain). 4-acetamido-2,2,6,6-tetramethyl-piperidine-1-oxyl (4-AcNH-TEMPO, CAS: 14691–89-5) and O,O′-1,3-propanediylbishydroxylamine (PDHA, w. BCCB7801, 98 %) obtained from Sigma-Aldrich (Czechia), ethanol (96 %, Cat.No.: 20025-A96-M1000) and sodium bromide (NaBr, 99.8 %, Cat.No.:30006-APO-G0500–1) from Lach-ner (Czechia).

Aldehyde-modified Chondroitin Sulphate (CSOX) was synthesized according to a method established (Bobula et al., 2016) with modifications (Fig. 2). In this process, CS (1040 mg) was dissolved in deionized

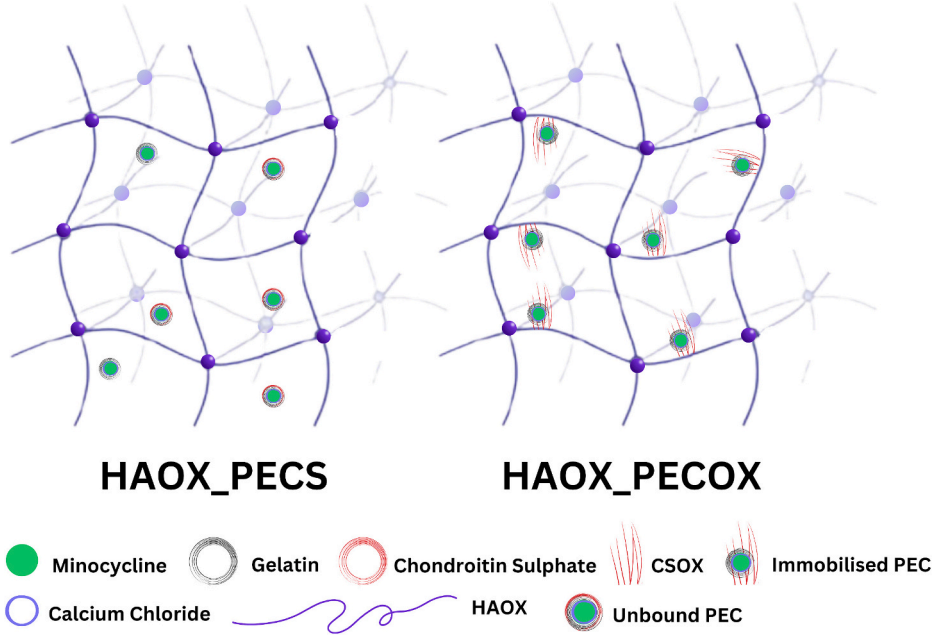

Fig. 1. HAOX-based Drug Delivery System: HAOX hydrogel containing unbound – and immobilized PEC.

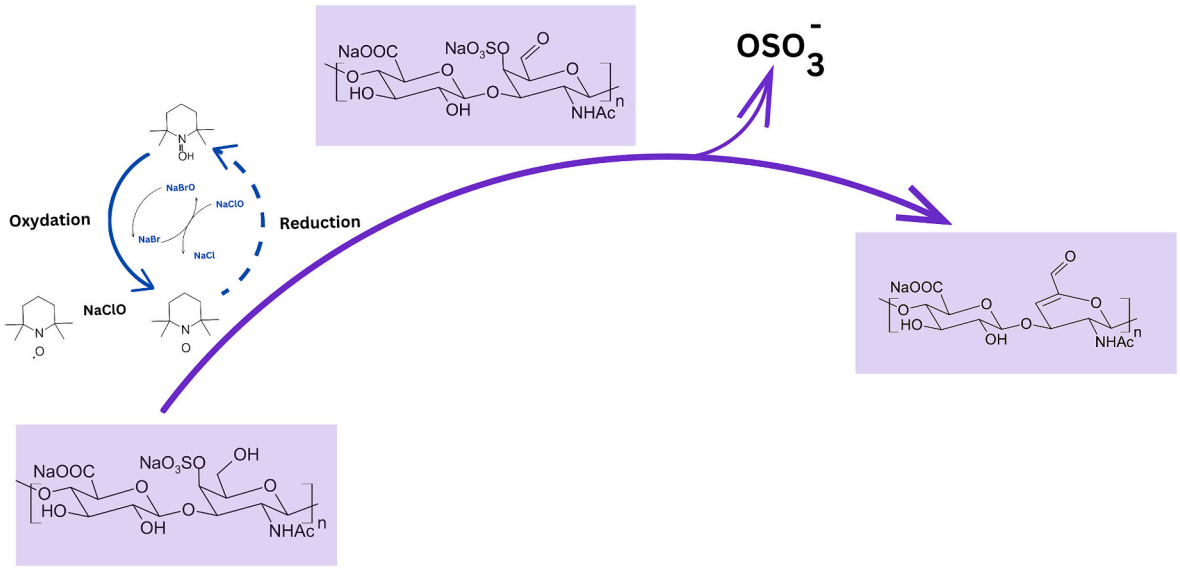

Fig. 2. One-pot synthesis of aldehyde-modified Chondroitin Sulphate (CSOX).

water (2 % *w/v*) containing disodium phosphate (400 mg) and NaBr (103 mg). A catalyst, 4-AcNH-TEMPO (4 mg), was introduced, and the reaction mixture was cooled to 5 °C. Subsequently, NaClO (560 μL, acive chlorine of 11 %) was added, and the solution was stirred at 5 °C for 30 min. The reaction was quenched by adding ethanol (5 mL). The resulting product was purified by dialysis (using a membrane with a molar mass cut-off of 14 kDa) against deionized water, followed by lyophilization.

The degree of functionalization (DF) for CSOX was assessed using ^{1}H NMR spectroscopy (Bruker Avance Neo 700 MHz) with 1 % (*w/v*) in D2O solutions. The spectra were analyzed using the SpinWorks software. DF was determined as the molar ratio of H6 proton at 9.21 ppm or H4 proton at 6.296 ppm to the protons of methyl group in GalNAc at 2.02 ppm, multiplied by 100 % (Eq. (1)).

$$DF = \frac{I_{-CHO}}{I_{-CH_3}} \times 300 \times 100\% \quad (1)$$

where I_{-CHO} is an integral of the signal at 9.217 ppm or 6.296, corresponding to -CHO of modified GalNAc subunit; I_{-CH_3} is an integral of the signal at 2.041 ppm, corresponding to -CH_3 of GalNAc.

The molar mass of CSOX (M_{CSOX}) was determined using SEC-MALLS following (Bobula et al., 2018). The experimental procedure involved injecting a volume of 100 μL of 2 % (w/v) CSOX dissolved in 0.9 % saline. Separation was conducted utilizing two sets of column series of PL aquagel-OH 40 (7.5 × 300 mm, 8 μm) and PL aquagel-OH 20 (7.5 × 300 mm, 5 μm), thermostated at 40 °C. The mobile phase consisted of 0.1 M sodium phosphate buffer (pH adjusted to 7.5) supplemented with 0.05 % NaN3, with a flow rate maintained at 0.8 mL min^{-1}, unless specified otherwise. The chromatographic system used in the experiment comprised of the Alliance e2695 HPLC, UV/Vis detector 2489, refractive index detector 2414 (Waters), and miniDAWN TREOS light scattering photometer (Wyatt Technology Corporation). Data acquisition and M_{CSOX} calculations were then performed using ASTRA software

(version 5.3.4, Wyatt Technology Corporation, USA).

2.1. Hydrogel preparation

All hydrogel formulations followed a standardized procedure involving the covalent cross-linking of aldehyde groups from either HAOX or CSOX with PDHA. The procedure involved dissolving the components in saline, adjusting the pH of the PDHA solution to 7 using NaOH, and utilizing a two-component system with connected syringes for cross-linking process (Supplementary information Fig. 1s). The detailed formulation is as follow:

2.1.1. Preparation of HAOX-based hydrogel and CSOX-based hydrogel

The process was initiated by dissolving HAOX and CSOX separately in saline at 60 °C for 3 h, followed by overnight stirring at 25 °C. Simultaneously, PDHA (150 mg) was dissolved in 10 mL of saline at 25 °C, with pH adjustment to 7 using NaOH. This preparation involved a two-component system, where two syringes were connected via a luer lock adapter. The first syringe contained the HAOX or CSOX solution, and the second syringe contained the minocycline and PDHA solution. The contents of these syringes were mixed in an 80:20 ratio and subsequently transferred into a Teflon mold. The ratio of polymer derivatives to PDHA can be adjusted based on the desired ease of injection.

2.1.2. Preparation of HAOX containing unbound PEC (HAOX_PECS)

HAOX_PECS was synthesized by dissolving HAOX, CA, GA, and CS in saline for 3 h at 60 °C, followed by stirring overnight at 25 °C. The cross-linking process utilized a dual-syringe system connected by a luer lock adapter. The first syringe loaded the polymer components, while the second syringe contained minocycline mixed with the cross-linking agent PDHA (Table 1). Achieving a homogenous mixture with a ratio of 80:20, the combined contents were transferred into a Teflon mold, forming hydrogels containing 200 μg mL^{-1} minocycline.

$$C_{POA} = \frac{C_{HAOX}.V_{HAOX}.M_{PDHA}.DS_{HAOX}}{V_{PDHA}.P.P_p.M_{HAOX}} \quad (2)$$

The physicochemical properties of the hydrogels were tuned by maintaining a HAOX concentration of 20 mg mL^{-1}. The calculation for PDHA concentration for 1.1 and 1.2 considered only the cross-linkable groups of aldehyde and hydroxylamine, which were presented by the HAOX and PDHA, respectively. The ratio of cross-linkable groups was consistently 1:1 for all formulations (Fig. 3). The concentration of PDHA (C_{PDHA}) was calculated using Eq. (2) with C_{HAOX} as the polymer concentration (w/v) of HAOX in the first syringe, DS_{HAOX} as the HAOX substitution degree, P representing the ratio of aldehyde to hydroxylamine groups which is equal to 1, P_p for the number of hydroxylamine groups in PDHA (2), V_{HAOX} as the volume of HAOX solution in the first syringe, V_{PDHA} as the total volume of minocycline mixed with PDHA solution, M_{PDHA}as the molar mass of PDHA (179 g mol^{-1}), and M_{HAOX} as the molar mass of the HA disaccharide unit (400 g mol^{-1}).

2.1.3. Preparation of HAOX containing immobilized PEC (HAOX_PECOX)

The preparation of HAOX_PECOX involved the dissolution of HAOX, CA, GA, and CSOX in saline for 3 h at 60 °C, followed by overnight stirring at 25 °C. The subsequent cross-linking procedure utilized steps and techniques similar to the rest of the formulations. However, the concentration of the cross-linking used was different. The concentration of PDHA in HAOX_PECOX considered the presence of aldehyde groups from two different polymers, HAOX and CSOX, with the ratio of crosslink-able group for both aldehyde and hydroxylamine still consistently 1:1 (Fig. 3).

$$C_{POA} = \left(\frac{C_{HAOX}.V_{HAOX}.M_{PDHA}.DS_{HAOX}}{V_{PDHA}.P.P_p.M_{HAOX}}\right) + \left(\frac{C_{CSOX}.V_{CSOX}.M_{PDHA}.DS_{CSOX}}{V_{PDHA}.P.P_p.M_{CSOX}}\right) \quad (3)$$

The concentration of PDHA for HAOX_PECOX (C_{PDHA}) was calculated using Eq. (3). The quantities in the second parenthesis are CSOX analogs of those in the first parenthesis, with M_{CSOX} as the molar mass of CS disaccharide unit (600 g mol^{-1}).

2.2. Gelation time

The time of gelation of HAOX was investigated using Discovery Hybrid Rheometer–3 (TA Instruments) in a plate-plate setup (40 mm diameter plate, 400 μm gap). After adding the cross-linking agent, real-time elastic (G′) and viscous (G″) moduli were determined. Viscoelastic properties were analyzed with a 180 s oscillatory time sweep at 25 °C, 5 % constant strain, 6.283 rad s^{-1} (1.0 Hz) angular frequency, and a 6 s sampling interval. Then, 0.8 mL gel-forming solution was placed on the Peltier plate, adding 200 μL PDHA solution containing minocycline. A 2000 s^{-1} pre-shear for 3 s homogenized the solutions and initiated gelation. At the crossover points of G′ and G″ curves, gelation time indicates the transition from viscous to elastic behavior. Measurements were repeated thrice, and averages with standard deviations were calculated.

2.3. Swelling ratio

The swelling ratio (Q) of the HAOX hydrogels was calculated using Eq. (4):

$$Q = \frac{(m_t - m_r)}{m_r} \text{ x } 100\% \quad (4)$$

where m_t is a mass of the hydrogel after swelling; m_r is a mass of the hydrogel in the relaxed state before swelling. The delivery system of HAOX-MN, CSOX-MN, HAOX_PECS, and HAOX_PECOX was transferred into a Transwell insert, with 2 mL saline as swelling medium. The change in sample's weight was determined after 1, 3, 7, 10, and 14 days of swelling. All experiments were performed at the temperature of 37 °C.

2.4. Minocycline release experiment and release fitting model

To investigate the in vitro release of minocycline from the hydrogels, we used the Transwell® drug release method. The hydrogel (1 mL) was transferred onto a semi-permeable polyester supporting membrane (25 mm in diameter; 3 μm pore size) on the donor compartment of the Transwell® insert (Corning, Inc., Acton, MA), while the Transwell® base

Table 1
The formulation studied for designing a suitable delivery system.

Formulations	HAOX (mg mL^{-1})	CSOX (mg mL^{-1})	CS (mg mL^{-1})	CA (μM)	GA (mg mL^{-1})	PDHA (mg mL^{-1})	Minocycline (μg mL^{-1})
HAOX	20	–	–	–	–	0.32	–
HAOX-MN	20	–	–	–	–	0.32	200
CSOX-MN	–	100	–	–	–	1.865	200
HAOX_PECS (unbound PEC)	20	–	5	7.2	1	0.32	200
HAOX_PECOX (immobilized PEC)	20	5	–	7.2	1	0.462	200

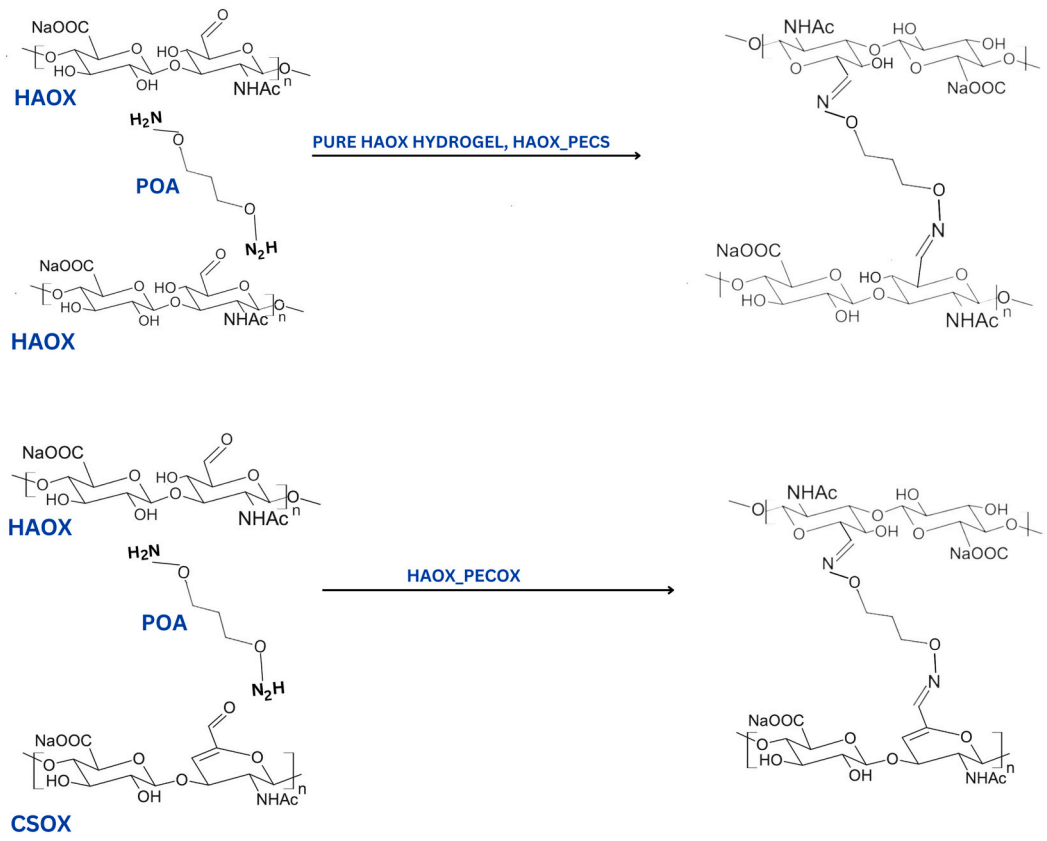

Fig. 3. Schematic illustration of the structure of cross-linked HAOX-based DDS, covering PURE HAOX and HAOX_PECS (upper reaction), and HAOX_PECOX (bottom reaction).

contained 2 mL of saline as the release medium. The entire Transwell® system was placed in an incubator (Witeg Wisd Incubator, WITEG Labortechnik) maintained at 37 °C and near 96 % relative humidity. At predetermined time points, the release medium was aspirated completely from the receptor compartment, which was immediately replenished with 2 mL of fresh saline solution post-sampling. The amounts of minocycline in the release medium was determined using HPLC (Acquity UPLC Waters, PDA-QDA). The amount of minocycline released was defined by cumulative drug release (CDR) eq. (5).

$$\mathrm{CDR} = \frac{m_t}{m_\infty} \text{ x } 100\% \tag{5}$$

m_t represents the mass of drug released at a specific interval, while m_∞ denotes the total mass of loaded drug. Korsmeyer–Peppas model was employed to identify the release mechanism of minocycline (Eq. (6)) (Korsmeyer et al., 1983).

$$\mathrm{k}t^n = \frac{m_t}{m_\infty} \tag{6}$$

With the aid of the model, we were able to both the release exponent (n) and the kinetics constant (k), which encompass the system's structural and geometric features.

2.5. Injectability

To assess the ease of the injection process, we employed needles sized 20 G with a length of 40 mm. The choice of needle dimensions was informed by the standard usage patterns among healthcare professionals, aiming to replicate the common practices in the field. We employed a two-component system of two syringes connected by a luer lock adapter to prepare the hydrogels. The first syringe contained a solution of HAOX with CA, GA, and CSOX, while the second syringe contained an minocycline solution mixed with the PDHA. After mixing the contents in the ratio of 80:20 for 10 s, we set the syringe on the machine. We assessed the injectability of cross-linked HAOX_PECOX using a Single Column Materials Testing System Instron 3342 at RT. The injection force was evaluated using a compression plate with a capacity of 100 N and a testing speed of 50 mm min^{-1}. The Bluehill software was used to collect data on the injection force, plunger displacement, and the dynamic glide force (*DGF*) and F_{max} values were calculated. We conducted each measurement at least three times, and the results were presented as average values with standard deviations.

2.6. Elastic limit and strain limit

The viscoelastic characteristics of hydrogels were characterized using the Discovery Hybrid Rheometer–3 manufactured by TA Instruments. All measurements utilized a 20 mm diameter crosshatched surface stainless-steel plate configuration to prevent hydrogel slippage. The experiments were conducted at 25 °C. Strain sweep oscillatory tests were performed to evaluate viscoelastic properties of hydrogels. The primary objective of the strain sweep examination was to ascertain the limit (γL) of the linear viscoelastic region (LVE) and establish the values of the elastic (G′) and viscous (G″) moduli within this specific LVE domain. This methodology was designed to analyze the response of G′ and G″ moduli in samples subjected to sinusoidal oscillatory strain at a consistent frequency and progressively escalating amplitude. The angular frequency was precisely set at 6.28 rad s^{-1} (equivalent to 1 Hz), and the oscillation displacement range was deliberately adjusted within the 0.001 to 2.0 rad range. γL within the LVE was identified as the strain value at which G becomes strain (stress) dependent. It is worth noting that the permissible deviation range for G' around the plateau value did not exceed ±5 %. The determination of G′ and G" values for the hydrogels was computed as the mean of the G′ values observed within

the LVE region.

2.7. M_c, mesh size, and cross-linking density

The influence of PEC in the formation of the hydrogel structure was analyzed by defining M_c by Peppa (Peppas et al., 2000) and mesh size using rubber elasticity theory derived by Flory (Flory, 1953). This theory detailed swelling-structure relationship. M_c correlates with Mesh size (ξ) defining the correlation distance between two adjacent cross-links in a swollen hydrogel. Still derived from the same Flory theory, ξ was calculated using the eq. (7):

$$\xi = l v_{2,s}^{-\frac{1}{3}} \left(\frac{2C_n M_c}{M_r}\right)^{\frac{1}{2}} \quad (7)$$

The virtual bond length, denoted as l, is defined as the distance from one glycosidic oxygen to another, spanning a monosaccharide (0.52 nm for HAOX (Martini et al., 2016), 0.96 nm for CSOX (Tanaka, 1978)); C_n is the Flory characteristic ratio (27 for HAOX (Martini et al., 2016), 15.705 for CSOX (Tanaka, 1978)), M_r is the molar mass of the repeat disaccharide unit (400 g mol^{-1} for HA, 600 g mol^{-1} for CSOX). For the M_c and ξ for immobilized PEC formulation, the contribution of CSOX structure in those two values was defined based on the volume fraction of the monomer presented in gel. The calculation process for ξ, including the determination of $\nu 2,s$ and M_c, is detailed in the Supporting Information.

2.8. Whole blood monocytes activation test (WB-MAT)

The Whole Blood Monocytes Activation Test (WB-MAT) was used to assess the bioactivity of minocycline released from the DDS, following established protocols with some modifications (Campbell et al., 2011; Pang et al., 2012). All individuals provided informed consent prior to donating blood. Initially, blood samples were collected from three healthy volunteers into sterile heparinized tubes labelled A, B, and C.

To stimulate Interlukin-6 (IL-6) expression, a stock solution of Lipopolysaccharide (LPS) stock solution was diluted with normal saline to concentrations of 5, 1, and 0.25, IU mL^{-1}. 100 μL of each LPS concentration was then applied in separate sterile Eppendorf and combined with 1000 μL of saline solution.

To assess minocycline bioactivity, the release medium from the DDS underwent HPLC analysis to determine the minocycline concentration. This was followed by dilution to approximately 5 μg mL^{-1} with normal saline. Subsequently, 1000 μL of each sample was transferred to a sterile Eppendorf, and 10 μL of either 2.5 IU mL^{-1} LPS or 10 IU mL^{-1} LPS was added.

Then, 100 μL of fresh heparinized blood was added to each Eppendorf (blood from each volunteer versus each LPS concentration and each sample of the release medium from the DDS), gently mixed, and incubated at 37 °C overnight. After gentle inversion, the solution underwent centrifugation at 13000 rpm for 10 min. The supernatant was transferred to a new Eppendorf, and IL-6 levels were measured using an ELISA kit in accordance with the manufacturer's instructions. Absorbance reading was taken using an Ensight Multimode Reader and analyzed with Kaleido software from PerkinElmer, Waltham, USA.

2.9. Data and statistics analysis

Statistical analyses involved one-way analysis of variance (ANOVA), and Student's *t*-test. A significance level of $p < 0.05$ was used to determine statistical significance. A Pearson correlation test and Linear regression were conducted to assess the presence of a statistically significant linear relationship between the two continuous variables.

3. Results and discussion

Aldehyde derivative of hyaluronic acid was selected as a basic structural component of the hydrogel matrix for the DDS. The versatility and biocompatibility of HAOX make it a suitable choice for developing hydrogel matrices for DDS. A key advantage lies in the aldehydic groups present in the HAOX structure, which are accessible for efficient cross-linking with various aminooxy compounds, such as PDHA (Alonso et al., 2021; Buffa et al., 2015). This cross-linking efficiency contributes to enhanced mechanical stability and a noticeable low in swelling, thereby maintaining structural integrity and ensuring consistent drug release without compromising the matrix (Buffa et al., 2015; Toropitsyn, Ščigalková, Pravda, & Velebný, 2023). Transitioning from selecting HAOX as the hydrogel matrix, the synthesis of CSOX emerges as pivotal step to form immobilized PEC integrated into the DDS. This synthesis introduces distinct attributes shaping the DDS's behavior for the delivery.

3.1. Synthesis of aldehyde-chondroitin sulphate

CS was modified to CSOX for the preparation of immobilized PEC. The one-pot synthesis of CSOX was conducted through regio- and chemoselective oxidation using Tempo/NaClO/NaBr, following the established protocols (Bobula et al., 2016). This oxidation specifically targeted the primary hydroxyl group at position C-6 of the D-galactosamine subunit (GalNAc) of CS, converting it to its unsaturated form. To identify the intermediate and confirm the CSOX structure, ^{1}H NMR analysis was employed on proton signals at positions C-4, C-6, and the saturated carboxyl with chemical shifts at 6.296 ppm, 9.217 ppm, respectively (Fig. 4). The results indicated that oxidation with 0.5 M equivalent of NaClO led to an approximate DF of 20 %. Additionally, M_{CSOX} was determined as 12 KDa using SEC-MALLS. CS modification by the one-pot synthesis method (Bobula et al., 2016) presents an efficient and well-controlled approach for producing CSOX. The method streamlines the synthesis process, saving time and reducing complexity (Bobula et al., 2016) without inducing ring-opening cleavage. This outcome demonstrates the precision and effectiveness of the method in the modification of the CS.

3.2. Gelation time

This study aims to create an injectable hydrogel that forms in situ and incorporates PEC for potential use in implanted devices or host tissue. The key focus is achieving precise control over the gelation time to facilitate easy injection and prevent leakage while ensuring the desired stability. Fig. 5 demonstrates how PEC influences the gelation time of HAOX-based DDS. The gelation times for various formulations, including PURE HAOX, HAOX-MN, HAOX_PECS, and HAOX_PECOX, were similar, all within a minute, indicating a rapid gelation process ($p > 0.05$) (Toropitsyn, Ščigalková, Pravda, & Velebný, 2023). In contrast, the pure CSOX hydrogel exhibited three times slower gelation time than other formulations ($p < 0.0001$).

The molecular complexity of CSOX as a low molar mass polysaccharide contributes to inherently slowing down the gelation process and prolonging it to 160 s. Slow gelation may lead to the release of minocycline and CSOX into the surroundings, potentially resulting in a less dense network structure and cargo loss (Y. Sun et al., 2020). This compromise in mechanical strength and stability necessary for certain applications. Therefore, CSOX-MN is not the suitable candidate for applications that require rapid and robust hydrogel formation. However, it is worth noting that the cross-linking of HAOX aligns with findings from a prior study (Toropitsyn, Ščigalková, Pravda, & Velebný, 2023), which showed a relatively fast rate of hydrogel formation within a minute. Additionally, the addition of unbound or immobilized PEC to the hydrogel structure can modify the network formation, leading to alterations in the gelation time (Novoskol'tseva et al., 2009; Rosas-Durazo et al., 2011). However, our results did not support this theory, as no significant differences were observed between the various formulations tested. Several investigations emphasize that a gelation period of one

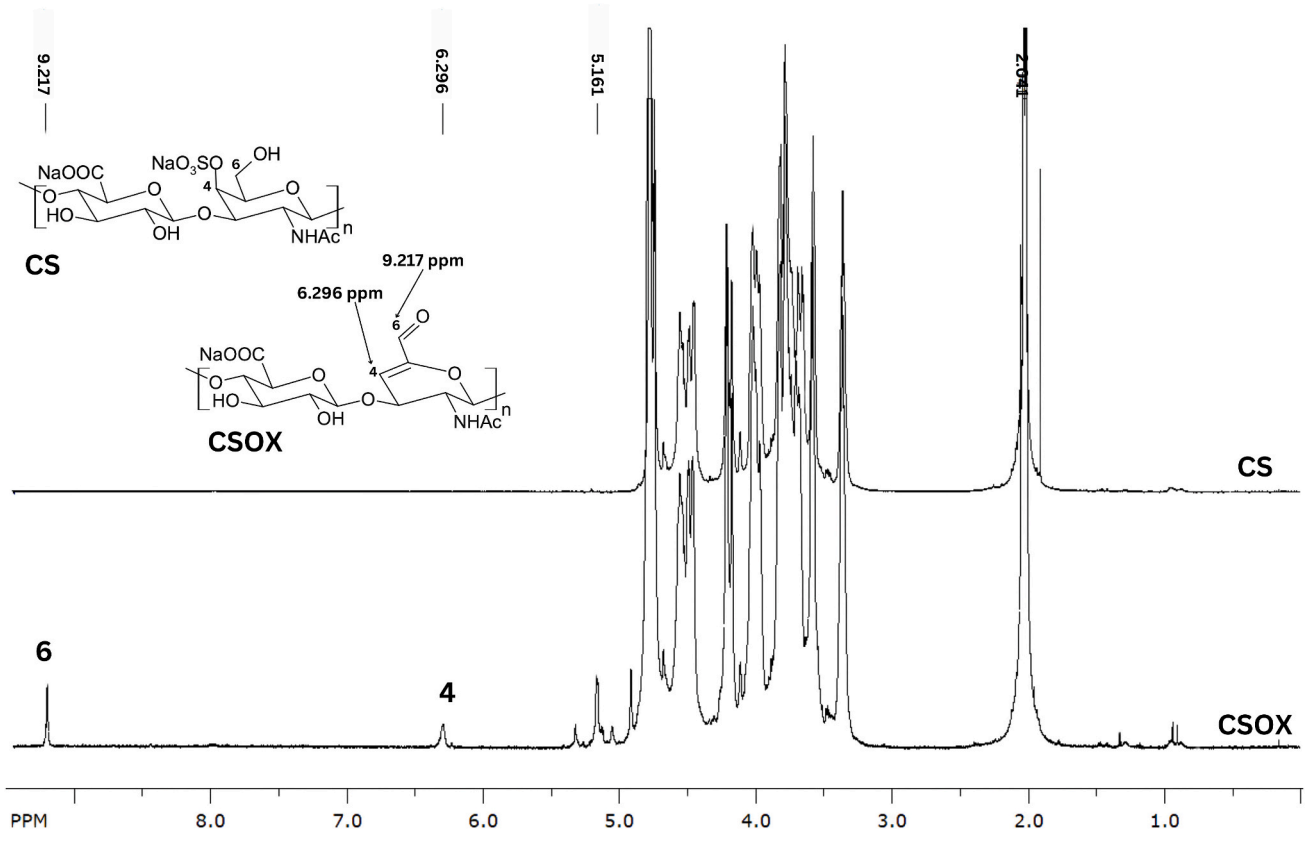

Fig. 4. ^{1}H NMR profile of CS and CSOX.

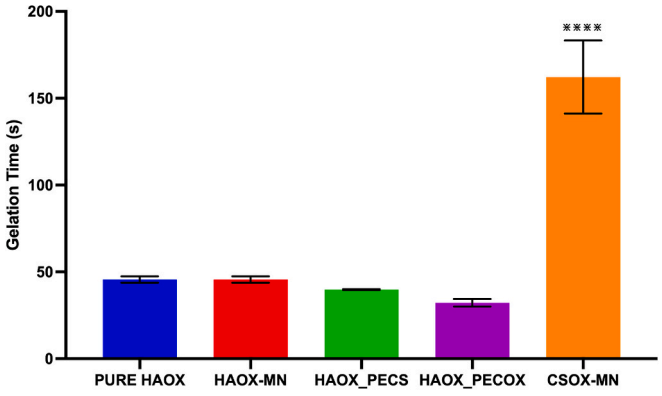

Fig. 5. Gelation time for hydrogels based on CSOX, HAOX, unbound – and immobilized PEC ($n = 3$, **** $p < 0.0001$ for CSOX-MN versus PURE HAOX).

minute is adequate for HAOX matrices to conform easily to the cavity's shape, ensuring a favorable fit and interface within tissues. Nevertheless, excessively rapid gelation could prematurely solidify, potentially leading to fluid retention within the needle (Y. Sun et al., 2020; Toropitsyn, Ščigalková, Pravda, & Velebný, 2023).

3.3. Swelling ratio

Assessing of the swelling ratio in cross-linked hydrogels has emerged as a critical factor for evaluating cross-linking efficiency (Xue et al., 2020). Low-swellable and non-swellable hydrogels are preferable for drug delivery applications (Xue et al., 2020), as they allow precise control over minocycline release kinetics. We evaluated the swelling behavior of PURE HAOX, CSOX-MN, HAOX-MN, HAOX_PECS, and HAOX_PECOX by measuring the change in sample weight after immersion in saline. Fig. 6 illustrates the dependence of the delivery system's swelling ratio on time, including the equilibrium swelling ratio.

The initial 24 h of swelling can be attributed to the leaching of unreacted materials within the hydrogel structure. This initial period resulted in a reduction in weight for all formulations but CSOX-MN. Notably, CSOX-MN exhibited an increase in weight since day one. This can be attributed to a higher concentration of sulphate groups (Bryant et al., 2004; Servaty et al., 2001) and polymer. The CSOX structure expanded beyond the insert and disintegrated within a week. This presents a significant limitation for minocycline release due to the highly hydrophilic nature of the highly swollen cross-linked CSOX-MN

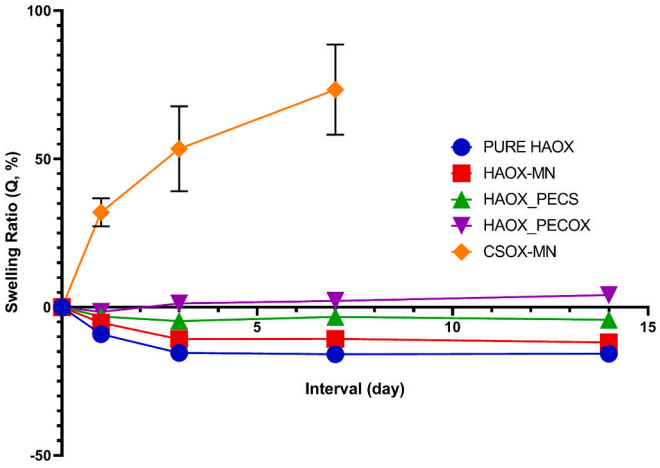

Fig. 6. The swelling ratio of hydrogels based on CSOX and HAOX containing minocycline, unbound PEC and immobilized PEC as function of time ($n = 3$).

formulation (Bobula et al., 2016). This can result in rapid water absorption, which in turn decelerates minocycline release, rather than controlling it through fluid exchange. Additionally, the swollen CSOX hydrogel puts undue pressure on the surroundings, which can lead to stress localization and accelerate structural degradation(Novoskol'tseva et al., 2009).

Following this initial phase, the optimal time to reach the equilibrium swollen state was seven days. The swelling capacity was directly related to cross-linking efficiency. Hydrogels containing HAOX-based polymer networks (PURE HAOX, HAOX-MN, and HAOX_PECS) exhibited comparable swelling behavior, indicating that minocycline and unbound PEC components did not significantly impact the cross-linking reaction. In contrast, hydrogel based on the mixed-polymer network created by the cross-linking of HAOX and CSOX derivatives (HAOX_PECOX) showed an increase in water uptake compared to the pure hydrogel ($p < 0.0001$). Conjugation of CSOX molecules to the polymer network of HAOX hydrogel enhanced water uptake due to additional hydration of the sulphate groups (Samantray et al., 2021).

Since HAOX-based hydrogels exhibit minimal structural expansion, drug diffusion from the hydrogel matrix proceeds in a controlled manner. This controlled release profile is beneficial for achieving sustained and predictable drug delivery over an extended period. The findings align with a previous study (Buffa et al., 2015; Toropitsyn, Ščigalková, Pravda, & Velebný, 2023), which indicated that the swelling ratio of HAOX-MN, HAOX_PECS, or HAOX_PECOX remains considerably low, ranging from 0 % to 1 %. Consequently, these hydrogels can be classified as very low-swellable, emphasizing their restrained swelling behavior. It is worth noting that our experimental setup involved confining the hydrogels within the Transwell® insert to mimic an implanted reservoir. A similar experiment found that confinement restricts gel exposure to surrounding fluid, particularly in Transwell®, where interaction occurs only at the bottom. This one-sided swelling lowers water absorption, led to asymmetric behavior in the kinetics of swelling and deswelling (G. Lin et al., 2009; Mihajlovic et al., 2022). Chemically, the presence of crosslinking junctions combined with confinement acts as a retractive force, counterbalancing the structural extension caused by swelling (Dulong et al., 2004; Shimojo et al., 2015).

3.4. Minocycline release experiment

Three different hydrogel formulations with varying methods for minocycline entrapment were prepared, omitting the CSOX-MN due to structural `instability. The release experiment used a Transwell® insert to replicate conditions similar to those in the implanted reservoir. HPLC was used to determine the minocycline release rate. The control hydrogel, HAOX-MN, exhibited an initial burst release within the first 24 h, followed by a slower release up to 120 h and a stable release up to 288 h, accounting for nearly 50 % of its total minocycline content (Fig. 7). HAOX_PECS, containing unbound PEC, demonstrated non-significant differences at all time points ($p > 0.05$), releasing approximately 30 % of the total minocycline over 288 h. Conversely, HAOX_PECOX, with immobilized PEC, significantly reduced burst release within 24 h to 88 % ($p < 0.01$) of the total minocycline loaded. Compared to HAOX-MN, immobilized PEC decreased burst release by up to 71 %, extending the release period to 19 days (data presented up to 288 h). The time taken for a 50 % release of minocycline (T50%) functions as a parameter indicating the hindrance in release. This duration is approximately 32 h for HAOX-MN, 57 h for HAOX_PECS, and 127 h for HAOX_PECOX.

The immobilized PEC in the hydrogel provides a stable environment for entrapped minocycline, preventing immediate release. This controlled release minimizes burst, which is crucial for avoiding side effects and ensuring prolonged therapeutic effectiveness. The release rate is closely tied to the type of PECs used. For HAOX-MN and HAOX_PECS, the observed release profile indicates that minocycline or complexed- minocycline is smaller than the hydrogel mesh size,

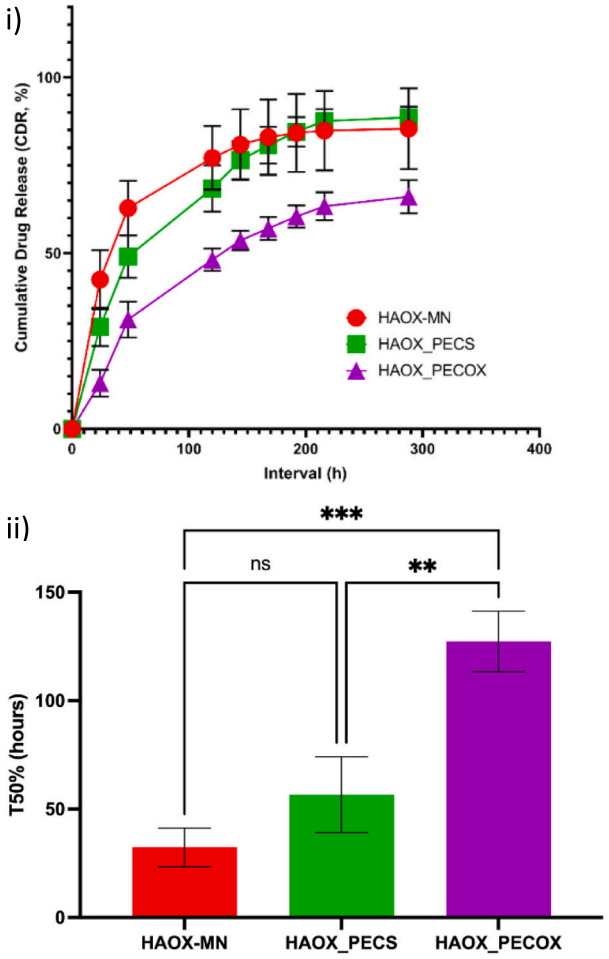

Fig. 7. Release profile of minocycline across different DDS formulation, i) Cumulative release of minocycline from CSOX and HAOX hydrogels containing minocycline unbound PEC and immobilized PEC as a function of time, ii) T50%. ($n = 3$,** $p < 0.01$, *** $p < 0.001$, ns is non-significant).

resulting in nearly 100 % drug release. This allows rapid interaction with the environment. HAOX_PECS may be beneficial for managing acute MS conditions, with a high initial burst, while HAOX_PECOX could be advantageous for stable and prolonged drug release in chronic conditions.

We employed the Korsmeyer-Peppas (Korsmeyer et al., 1983) model to analyze the release rate of minocycline and subsequently determined the kinetic constants (k) and exponents (n), which can be found in Table 2. Across all datasets, the coefficient of determination (R^2) consistently fell within the range of 0.993 to 0.997. The lowest values for k were associated with a more hindered release of minocycline from the HAOX_PECOX, followed by lower k values for the release from HAOX_PECS. The highest k values were recorded for minocycline release from the HAOX-MN. The release of minocycline from HAOX-MN and HAOX_PECS is mainly controlled by Fickian diffusion represented by $n < 0.5$ (Korsmeyer et al., 1983). (See Table 2.)

On the other hand, the release mechanisms of HAOX_PECOX is

Table 2
k and n calculated using the Korsmeyer–Peppas equation.

Formulations	k	n	R^2
HAOX-MN	0.168	0.318	0.995
HAOX_PECS	0.075	0.463	0.997
HAOX_PECOX	0. 027	0.595	0.993

classified as anomalous transport as n falls between 0.5 and 1. The variability in minocycline release rates is likely attributed to distinct interactions within the hydrogel network and with the PEC. This finding aligns with prior research indicating diverse minocycline release rates from HA, underscoring an interplay between both structures that impacts release kinetics (Miyazaki et al., 1995). Further modeling is crucial for understanding PEC and PEC-HAOX decomplexation as the interaction is influenced by the charge states of the components, which in turn respond to the local environment. Experimental evidence indicates that counterion release is a significant factor, which can be affected by the charge density and drug affinity for the polymer matrix, (Achazi et al., 2021; Gummel et al., 2007), while PEC stability may also affect drug release kinetics.

Pearson correlation between T50% and swelling profile also suggesting the presence of positive interrelated effect between the released minocycline and water uptake (refer to Fig. 3s in supplementary information). Experimentally, the rise in T50% seen in HAOX_PECOX may be attributed to the immobilization of CSOX, which is accountable for entrapping minocycline alongside the water absorption facilitated by immobilized sulfate groups. Furthermore, it is established that minocycline exhibits different release rates from PECs based on the binding affinity between components (Holmkvist et al., 2016; Wang et al., 2017; Wu et al., 2018; Zhang et al., 2014), with the understanding of dissociation kinetics remain unclear. Consequently, it can be inferred that the release of minocycline from HAOX-based hydrogels is influenced by two pivotal factors: the rate of dissociation from PEC and the interactions of minocycline with the hydrogel network.

3.5. Injectability

In this study, selecting an appropriate needle-syringe system ensure a smooth injection process. Injectability, denoting the ease of injection, is primarily assessed through the measurement of injection force (Alonso et al., 2021), It is gauged by analyzing the maximum force (F_{max}), which corresponds to the highest force exerted before complete extrusion, followed by a pronounced decline in the *DGF*. The *DGF* represents the consistent force needed to sustain fluid movement out of the syringe. During injectability tests, a constant crosshead speed of 50 mm s^{-1} was maintained while examining the impact of needle diameter. Our findings reveal that the pre-crosslinked formulation is still injectable with 20 G needle (see Table 3). Importantly, all *DGF* values obtained for needle sizes of 20 G remain below 40 N, signifying the fall within an acceptable range (Alonso et al., 2021).

3.6. Viscoelastic properties

Analyzing the rheological properties of formulations provides insights into their physical characteristics, stability (Kopač et al., 2022), and potential impact on drug release rates. Oscillation amplitude strain tests were conducted to assess the impact of PEC on the structural properties of HAOX hydrogels and variants (HAOX-MN, HAOX_PECS, and HAOX_PECOX) (see Fig. 8). The strain sweep tests confirmed gel-like behavior in all hydrogels (Kopač et al., 2022), as indicated by consistently higher G' compared to G". The materials exhibited a solid structure with a tan δ of <0.1 at 1 Hz in the LVE range. Evaluating durability using G' revealed comparable strength in HAOX-MN and HAOX_PECOX to PURE HAOX. However, unbound PEC significantly impacted HAOX hydrogels, resulting in a 25 % reduction in G' and increased brittleness, possibly due to inhomogeneity (T. L. Sun et al., 2013; Takeno & Sato, 2016). Despite this, G' values (2200 to 3800 Pa) align with hydrogels for sustained drug release, ensuring stability against environmental factors. These robust hydrogels offer a stable environment for entrapped drugs, maintaining structural integrity and consistent dosing while allowing for structural flexibility (elasticity limits: 30–45 %, $p > 0.05$) which are corroborated with previously established results (Toropitsyn, Ščigalková, Pravda, & Velebný, 2023).

In certain scenarios, a negative correlation might exist between the Elastic limit (G') and swelling capacity of a hydrogel. This indicates that as the G' rises, reduces the swelling capacity. Such a relationship could arise from sufficient in the hydrogel's cross-linking density or polymer concentration, leading to reinforced network structures capable of withstanding deformation during the water intake (Ali et al., 2018; Gwon et al., 2017; Stojkov et al., 2021). Bivariate Pearson correlation from these two variables (see Fig. 4s on supplementary information) does not signify the presence of any dependency.

Table 3
Injectability based on measured DGF and Fmax from HAOX_PECOX.

Formulation	*Needle size*	***DGF*** (N)	F_{max} (Kpa)
PEC_CSOX	20 G × 40 mm	7.9 ± 0.6	576 ± 13

3.7. Cross-linking density, molar mass between cross-links (M_c) and mesh size (ξ)

ξ refers to the interstitial space between polymer chains which govern fluid retention and exchange (Ho et al., 2022; Li & Mooney, 2016b). Additionally, M_c correlates to network swelling capacity (Hoti et al., 2021). The cross-linking density of the hydrogel is intricately linked to both the M_c and ξ. An increase in cross-linking density often corresponds to a reduction in ξ and M_c, highlighting the interdependence of these structural parameters in hydrogel formation (Hoti et al., 2021). These parameters influence drug diffusion and the release kinetics.

The results presented in Table 4 reveal no significant differences in the cross-linking density of PURE HAOX and HAOX-MN. Meanwhile, including unbound and immobilized PEC has the opposite effect, reducing and increasing cross-linking density, respectively. Comparable crosslinking density demonstrate that the main building block of the polymer network is the long chain of HAOX. Meanwhile, although CSOX is present on the site for crosslinking in HAOX_PECOX, its short characteristics prevent it from contributing to effective chain formation. As a result, the swelling observed is comparable, leading to a mesh size of similar value. Furthermore, pure HAOX and HAOX-MN exhibit similar M_c values of 129,153 g mol^{-1} and 130,222 g mol^{-1}, respectively ($p > 0.05$). Notably, the presence of unbound PEC and immobilized PEC has a substantial impact on M_c. Unbound PEC increases M_c by 3 % to 132,832 g mol^{-1} ($p < 0.001$), while immobilized PEC reduces M_c by 27 % to 93,314 g mol^{-1} ($p < 0.0001$). Moreover, significant differences in ξ are observed between the pure hydrogel and the other formulations. Previous research indicated that the presence of bioactive substances entrapped in the HAOX structure could alter ξ by influencing cross-linking efficiency (Toropitsyn, Ščigalková, Pravda, & Velebný, 2023). Our results support this observation, showing that the introduction of minocycline leads to a 13 % reduction in ξ ($p < 0.001$), and unbound PEC results in a 9 % reduction ($p < 0.01$). Interestingly, the ξ in the presence of immobilized PEC is comparable to that of HAOX-MN ($p > 0.05$).

The findings indicate that immobilized PEC results in the lowest M_c among the formulations yet still has comparable ξ with PURE HAOX. This outcome can be explained by both the calculation method employed and the inherent characteristics of the polymers. In calculating M_c for DDS with immobilized PEC, the considerations involved incorporating characteristic values from HAOX and CSOX, rather than solely relying on the HAOX. For instance, the M_n value of CSOX (209,352 g mol^{-1}) calculated based on the Eq. (2) in supplementary information was considered alongside with the M_n from HAOX (300,000 g mol^{-1}). Furthermore, there is a significant disparity in ρ_p values, with 1,299,000 g m^{-3} for HAOX and 120,000 g m^{-3} used for CSOX. Mathematically, introducing lower value of M_n and ρ_p corresponds to a lower M_c. Additionally, CSOX tends to cross-link with CSOX

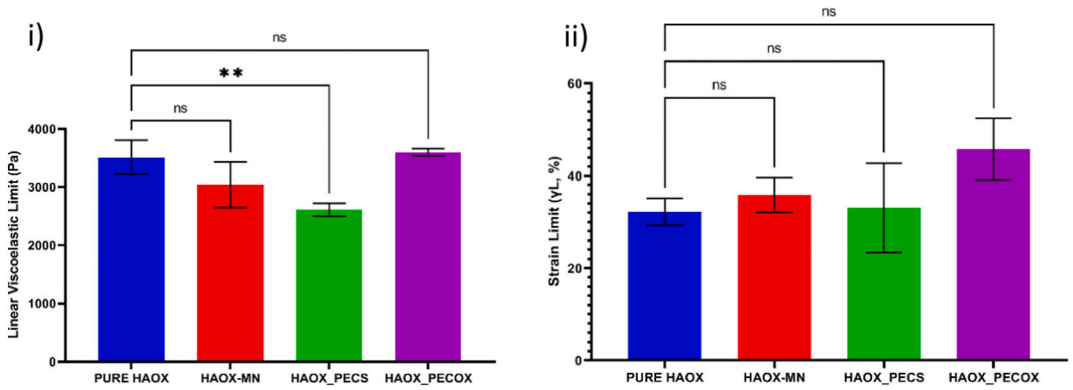

Fig. 8. Viscoelastic properties of hydrogels; i) G' (LVE) and ii) γ L of hydrogels based on HAOX containing minocycline, unbound PEC and immobilized PEC ($n = 3$, ** $P \leq 0.01$ HAOX_PECS vs PURE HAOX).

Table 4
Cross-linking density, M_c and ξ based on HAOX containing minocycline, unbound PEC and immobilized PEC.

Formulations	Cross-linking Density (mol mL^{-1})	M_c (g mol^{-1})	ξ (nm)
PURE HAOX	9.52 ± 0.02	(129.2 ± 0.4) × 10^3	317 ± 13
HAOX-MN	9.4 ± 0.1	(130.2 ± 1.3) × 10^3	275 ± 8
HAOX_PECS	9.25 ± 0.05	(132.9 ± 0.9) × 10^3	287 ± 4
HAOX_PECOX	13.49 ± 0.01	(93.3 ± 0.2) × 10^3	332 ± 2

than with HAOX, forming a branching structure instead of extending the cross-linking of the HAOX-CSOX network (Takeno & Sato, 2016), leading to an observed ξ that is comparable to PURE HAOX. The presence of sulfate groups, coupled with this branching, potentially creates more free volume, enhancing water affinity. Furthermore, the ξ value for HAOX hydrogels containing minocycline or PECs falls within the typical range of 100–400 nm observed in other HA-based hydrogels (Tao et al., 2012; Toropitsyn, Ščigalková, Pravda, Toropitsyna, & Velebný, 2023; Toropitsyn, Ščigalková, Pravda, & Velebný, 2023). This suggests that HAOX primarily influences the mesh size, and the short chain of CSOX is not effectively contributing to the network formation in the delivery system.

The Pearson correlation analysis uncovered a significant positive correlation between T50% and mesh size, contradicting traditional expectations (Fig. 6s supplementary information). While larger mesh size typically leads to faster drug release (J.Penn & Hennessy, 2022; Rehmann et al., 2017; Thang et al., 2023), our study revealed the opposite trend. This underscores the contributions of various factor influencing the drug diffusion within the DDS, including the water uptake (Fig. 3s supplementary information) and PEC dissociation, which emphasizes the necessity of a deeper understanding of underlying mechanisms.

Further validation for calculation M_c and ξ using Rubber Elasticity theory needs to be performed, considering the model's suitability to the nature of the studied DDS network. Flory's model of rubber elasticity assumes that all network junctions are tetrafunctional and does not consider for potential defects raised from complex polymer architectures (Richbourg & Peppas, 2020). Currently, there exists no method to directly measure ξ in the relaxed state. Consequently, all assessments of mesh size depend on correlation, with the most commonly used approach being the interpretation of swelling data (Richbourg & Peppas, 2020). The DDS network under investigations consists of polydisperse biopolymers with varying substitution groups distributions.

3.8. Whole blood monocytes activation test

IL-6 expressing monocytes are known to contribute to neuroinflammation in MS. Active relapsing-remitting MS patients have shown resistance to regulatory T cells due to IL-6 signaling, which can aggravate the disease (Janssens et al., 2015; Khan et al., 2023; Kim et al., 2024). Targeting the monocytes and IL-6 signaling with minocycline, an antibiotic known for its anti-inflammatory properties in the CNS (Henry et al., 2008), can be a potential strategy for treating MS. To assess the extent to which minocycline, when released from the delivery system, remains in an active state, we conducted experiments to measure the reduction in monocyte activation. In the first experiment, whole blood samples from three different volunteers were treated with LPS and then determined the production of IL-6. As shown in Fig. 7s (Supplementary information), increasing LPS concentration (0.25–5 IU mL^{-1}) correlates with the increase of IL-6 expression. This dose response study revealed significant difference between the effect of LPS at concentration 1 to 5 IU mL^{-1}, indicating that stimulation was already achieved at 1 IU mL^{-1}. The second experiment followed experimental conditions established in Fig. 7s (Supplementary information), in which we incubated blood samples with minocycline and subsequently stimulated the samples with 1 IU mL^{-1} LPS. Interestingly, minocycline reduced LPS-induced IL-6 secretion by up to 56 % (Fig. 9). This suggests that minocycline has a consistent inhibitory effect on IL-6 production. The obtained results confirmed the suitability of combination of HAOX hydrogels PEC as carriers of minocycline because encapsulated minocycline was released from the hydrogels through autonomous diffusion and maintained their biological activity to alter the expression of pro-inflammatory cytokines.

4. Conclusions

This article comprehensively describes the combination between PEC entrapping minocycline and hydrogels based on HAOX cross-linked by PDHA. Opposite charge attractions between PEC components and minocycline promoted the entrapment of minocycline within the structure. Two types of PECs were incorporated in the system, namely unbound PEC composed of minocycline, CA, GA, and CS, which was later referred to as HAOX_PECS. On the other hand, immobilized PEC formed by minocycline CA, GA, and CSOX, was referred to as HAOX_PECOX. The immobilization of the PEC structure was proceeded by the cross-linking process between HAOX and CSOX mediated by PDHA.

The results demonstrate that precursor gel mixtures containing minocycline -loaded PEC can be easily administered via a 1 mL syringes connected to a 20-gauge needle. Introducing of immobilized PECs into HAOX hydrogels did not impact the cross-linking reaction. Furthermore, the properties of these hydrogels can be tailored by adjusting the concentrations of HAOX and PDHA while carefully selecting suitable PEC components. This allows for the creation of low-swellable hydrogels containing minocycline with the desired viscoelastic properties, and the entire gelation process can be completed within minutes.

Additional findings corroborated the effectiveness of PEC-loaded

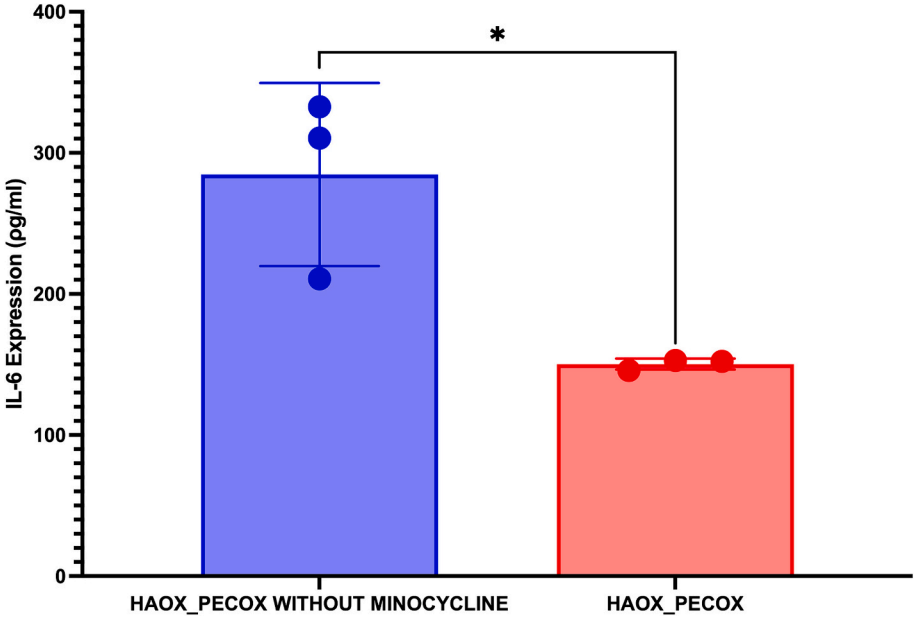

Fig. 9. Dose response for LPS treatment of whole blood monocytes activation after treatment with release medium from HAOX_PECOX and HAOX_PECOX without minocycline ($n = 3$, * $P \leq 0.05$).

HAOX hydrogels as reservoirs for minocycline due to the successful release of minocycline from the system while preserving its high bioactivity. The effect of different types of PECs was different release profile, with immobilized PEC able to reduce burst release and the subsequent of release of minocycline significantly. The application of the Korsmeyer-Peppas model revealed that the release mechanism of minocycline from PEC-loaded HAOX hydrogels, featuring ξ values within the range of 318–340 nm, followed Fickian diffusion for HAOX-MN and unbound PEC, and anomalous transport pattern for immobilized PEC. However, it's worth noting that the impact of ξ on the release rate of minocycline was not conclusively established. Notably, the released minocycline retained the ability to reduce IL-6 expression by 56 %.

Based on our findings, PEC-loaded HAOX is a potential drug delivery strategy over standard formulations such as nanoparticles (Dinarvand et al., 2012) or liposomal (Shamkani et al., 2023) due to its notable simplicity in formulation and preparation. Unlike the intricate processes involved in nanoparticles synthesis, the preparation of in situ PEC involves the straightforward interaction of oppositely charged polymeric components in tandem with the cross-linking process of HAOX/PDHA. This simplicity not only streamlines the manufacturing process but also enhances the reproducibility of the DDS. Also, we have devised a novel drug delivery approach that encompasses HAOX hydrogel and minocycline -loaded PEC suitable to be integrated in a reservoir. This approach capitalizes on the ability to create a combination of HAOX and PEC in situ. This in situ formation simplifies the transfer to an implanted reservoir, potentially extending the duration of minocycline release while preserving its biological activity.

Furthermore, the PEC-loaded hydrogel offers the advantage of injectability using a syringe. This is made possible by adjusting the viscosity and injection force of the pre-gelled solution. Simultaneously, this hydrogel provides a durable compartment for anchoring minocycline -loaded PEC thanks to its appropriate G' when formed in situ.

In our future research, we will prioritize investigating how the developed hydrogel affects the pyrogenicity and phenotype of other relevant cell types.

CRediT authorship contribution statement

Tutut Habibah: Writing – original draft, Investigation, Conceptualization. **Jana Matonohová:** Methodology, Investigation. **Jaromír Kulhánek:** Methodology, Investigation. **Una Fitzgerald:** Writing – review & editing, Validation, Project administration. **Marek Ingr:** Writing – review & editing, Supervision. **Martin Pravda:** Conceptualization. **Abhay Pandit:** Writing – review & editing, Supervision, Conceptualization. **Vladimír Velebný:** Writing – review & editing, Supervision, Conceptualization.

Declaration of competing interest

Vladimír Velebný has a financial interest in the company Contipro a. s., Dolní Dobrouč, Czech Republic, the commercial producer of hyaluronic acid, Martin Pravda is employee of Contipro a.s.

Data availability

Data will be made available on request.

Acknowledgements

This work was supported by the European Union's Horizon 2020 research and innovation programme under the Marie Skłodowska-Curie grant agreement No 813263.

Appendix A. Supplementary data

Supplementary data to this article can be found online at https://doi.org/10.1016/j.carbpol.2024.122455.

References

Achazi, K., Haag, R., Ballauff, M., Dernedde, J., Kizhakkedathu, J. N., Maysinger, D., & Multhaup, G. (2021). Understanding the interaction of polyelectrolyte architectures with proteins and Biosystems. In (International ed.,, *60. Angewandte Chemie* (pp. 3882–3904). Wiley-VCH Verlag. https://doi.org/10.1002/anie.202006457. Issue 8.

Ali, W., Gebert, B., Altinpinar, S., Mayer-Gall, T., Ulbricht, M., Gutmann, J. S., & Graf, K. (2018). On the potential of using dual-function hydrogels for brackish water desalination. *Polymers, 10*(6). https://doi.org/10.3390/polym10060567

Alonso, J. M., Del Olmo, J. A., Gonzalez, R. P., & Saez-martinez, V. (2021). Injectable hydrogels: From laboratory to industrialization. In , *13. Polymers* (pp. 1–24). MDPI AG. https://doi.org/10.3390/polym13040650. Issue 4.

Andravizou, A., Dardiotis, E., Artemiadis, A., Sokratous, M., Siokas, V., Tsouris, Z., … Hadjigeorgiou, G. M. (2019). Brain atrophy in multiple sclerosis: Mechanisms,

clinical relevance and treatment options. *Autoimmunity Highlights, 10*(1). https://doi.org/10.1186/s13317-019-0117-5

Asadi, A., Abdi, M., Kouhsari, E., Panahi, P., Sholeh, M., Sadeghifard, N., Amiriani, T., Ahmadi, A., Maleki, A., & Gholami, M. (2020). Minocycline, focus on mechanisms of resistance, antibacterial activity, and clinical effectiveness: Back to the future. In *journal of global antimicrobial resistance* (Vol. 22, pp. 161–174). Elsevier ltd. doi:https://doi.org/10.1016/j.jgar.2020.01.022.

Barone, D. A., Singer, B. A., Merkov, L., Rametta, M., & Suarez, G. (2016). Survey of US patients with multiple sclerosis: Comparison of the new electronic interferon Beta-1b autoinjector (BETACONNECT™) with mechanical autoinjectors. Neurology and Therapy, 5(2), 155–167. doi:https://doi.org/10.1007/s40120-016-0047-3.

Bobula, T., Buffa, R., Hermannová, M., Vágnerová, H., Doležková, I., & Velebný, V. (2018). The synthesis of a new unsaturated derivative of chondroitin sulfate with increased antioxidant properties. *Carbohydrate Polymers, 190*, 175–183. https://doi.org/10.1016/j.carbpol.2018.02.080

Bobula, T., Buffa, R., Procházková, P., Vágnerová, H., Moravcová, V., Šuláková, R., Židek, O., & Velebný, V. (2016). One-pot synthesis of α,β-unsaturated polyaldehyde of chondroitin sulfate. Carbohydrate Polymers, 136, 1002–1009. doi:https://doi.org/10.1016/j.carbpol.2015.10.005.

Bryant, S. J., Davis-Arehart, K. A., Luo, N., Shoemaker, R. K., Arthur, J. A., & Anseth, K. S. (2004). Synthesis and characterization of photopolymerized multifunctional hydrogels: Water-soluble poly(vinyl alcohol) and chondroitin sulfate macromers for chondrocyte encapsulation. *Macromolecules, 37*(18), 6726–6733. https://doi.org/10.1021/ma0499324

Buffa, R., Šedová, P., Basarabová, I., Moravcová, M., Wolfová, L., Bobula, T., & Velebný, V. (2015). α,β-Unsaturated aldehyde of hyaluronan - Synthesis, analysis and applications. Carbohydrate Polymers, 134, 293–299. doi:https://doi.org/10.1016/j.carbpol.2015.07.084.

Campbell, J. H., Burdo, T. H., Autissier, P., Bombardier, J. P., Westmoreland, S. V., Soulas, C., … Williams, K. C. (2011). Minocycline inhibition of monocyte activation correlates with neuronal protection in SIV NeuroAIDS. *PLoS One, 6*(4). https://doi.org/10.1371/journal.pone.0018688

Creta, A., Gilio, L., Centonze, D., & Fantozzi, R. (2022). Usability of an application device for nabiximols oromucosal spray in patients with upper limb impaired multiple sclerosis. *Neurodegenerative Disease Management, 12*(4), 195–201. https://doi.org/10.2217/nmt-2022-0014

Dinarvand, R., Jafarzadeh Kashi, T., Eskandarion, E.-M., Samadi, A., & F., & Eshraghi.. (2012). Improved drug loading and antibacterial activity of minocycline-loaded PLGA nanoparticles prepared by solid/oil/water ion pairing method. *International Journal of Nanomedicine, 221*. https://doi.org/10.2147/ijn.s27709

Dulong, V., Lack, S., Le Cerf, D., Picton, L., Vannier, J. P., & Muller, G. (2004). Hyaluronan-based hydrogels particles prepared by crosslinking with trisodium trimetaphosphate. *Synthesis and characterization. Carbohydrate Polymers, 57*(1), 1–6. https://doi.org/10.1016/j.carbpol.2003.12.006

Elewa, H. F., Hilali, R., Hess, D. C., Machado, L. S., & Fagan, S. C. (2006). Minocycline for short-term neuroprotection. *Pharmacotherapy, 26*(4), 515–521. https://doi.org/10.1592/phco.26.4.515

EMSP. (2021). MS Barometer 2020: Assessing the gaps in care for people with multiple sclerosis across Europe. http://msbarometer.com/.

Flory, P. J. (1953). *Principle of polymer chemistry*. USA: Cornell University Press.

Gajofatto, A., & Benedetti, M. D. (2015). Treatment strategies for multiple sclerosis: When to start, when to change, when to stop? *World Journal of Clinical Cases, 3*(7), 545. https://doi.org/10.12998/wjcc.v3.i7.545

Garrido-Mesa, N., Zarzuelo, A., & Gálvez, J. (2013). What is behind the non-antibiotic properties of minocycline? In *pharmacological research* (Vol. 67, issue 1, pp. 18–30). doi:https://doi.org/10.1016/j.phrs.2012.10.006.

Ghosh, B., Nong, J., Wang, Z., Urban, M. W., Heinsinger, N. M., Trovillion, V. A., … Zhong, Y. (2019). A hydrogel engineered to deliver minocycline locally to the injured cervical spinal cord protects respiratory neural circuitry and preserves diaphragm function. *Neurobiology of Disease, 127*, 591–604. https://doi.org/10.1016/j.nbd.2019.04.014

Gong, J. P., Katsuyama, Y., Kurokawa, T., & Osada, Y. (2003). Double-network hydrogels with extremely high mechanical strength. *Advanced Materials, 15*(14), 1155–1158. https://doi.org/10.1002/adma.200304907

Gummel, J., Cousin, F., & Boué, F. (2007). Counterions release from electrostatic complexes of polyelectrolytes and proteins of opposite charge: A direct measurement. *Journal of the American Chemical Society, 129*(18), 5806–5807. https://doi.org/10.1021/ja070414t

Gwon, K., Kim, E., & Tae, G. (2017). Heparin-hyaluronic acid hydrogel in support of cellular activities of 3D encapsulated adipose derived stem cells. *Acta Biomaterialia, 49*, 284–295. https://doi.org/10.1016/j.actbio.2016.12.001

Henry, C. J., Huang, Y., Wynne, A., Hanke, M., Himler, J., Bailey, M. T., … Godbout, J. P. (2008). Minocycline attenuates lipopolysaccharide (LPS)-induced neuroinflammation, sickness behavior, and anhedonia. *Journal of Neuroinflammation, 5*. https://doi.org/10.1186/1742-2094-5-15

Ho, T. C., Chang, C. C., Chan, H. P., Chung, T. W., Shu, C. W., Chuang, K. P., Duh, T. H., Yang, M. H., & Tyan, Y. C. (2022). Hydrogels: Properties and applications in biomedicine. In *molecules* (Vol. 27, issue 9). MDPI. doi:https://doi.org/10.3390/molecules27092902.

Holmkvist, A. D., Friberg, A., Nilsson, U. J., & Schouenborg, J. (2016). Hydrophobic ion pairing of a minocycline/Ca2+/AOT complex for preparation of drug-loaded PLGA nanoparticles with improved sustained release. *International Journal of Pharmaceutics, 499*(1–2), 351–357. https://doi.org/10.1016/j.ijpharm.2016.01.011

Hoti, G., Caldera, F., Cecone, C., Pedrazzo, A. R., Anceschi, A., Appleton, S. L., … Trotta, F. (2021). Effect of the cross-linking density on the swelling and rheological behavior of ester-bridged β-cyclodextrin nanosponges. *Materials, 14*(3), 1–20. https://doi.org/10.3390/ma14030478

Huang, X., Li, J., Luo, J., Gao, Q., Mao, A., & Li, J. (2021). Research progress on double-network hydrogels. *Materials today. Communications, 29*.

J.Penn, M., & Hennessy, M. G. (2022). Optimal loading of hydrogel-based drug-delivery systems. *Applied Mathematical Modelling, 112*, 649–668. https://doi.org/10.1016/j.apm.2022.08.008

Janssens, K., Slaets, H., & Hellings, N. (2015). Immunomodulatory properties of the IL-6 cytokine family in multiple sclerosis. *Annals of the New York Academy of Sciences, 1351*(1), 52–60. https://doi.org/10.1111/nyas.12821

Khan, A. W., Farooq, M., Hwang, M. J., Haseeb, M., & Choi, S. (2023). Autoimmune Neuroinflammatory diseases: Role of interleukins. In *international journal of molecular sciences* (Vol. 24, issue 9). Multidisciplinary digital publishing institute (MDPI). doi:https://doi.org/10.3390/ijms24097960.

Kim, M., Kim, W. S., Cha, H., Kim, B., Kwon, Y. N., & Kim, S. M. (2024). Early involvement of peripherally derived monocytes in inflammation in an NMO-like mouse model. *Scientific Reports, 14*(1). https://doi.org/10.1038/s41598-024-51759-4

Kopač, T., Abrami, M., Grassi, M., Ručigaj, A., & Krajnc, M. (2022). Polysaccharide-based hydrogels crosslink density equation: A rheological and LF-NMR study of polymer-polymer interactions. *Carbohydrate Polymers, 277*. https://doi.org/10.1016/j.carbpol.2021.118895

Korsmeyer, R. W., Gurny, R., Doelker, E., Buri, P., & Peppas, N. A. (1983). Mechanisms of solute release from porous hydrophilic polymers. In *international. Journal of Pharmaceutics, 15*.

Li, J., & Mooney, D. J. (2016a). Designing hydrogels for controlled drug delivery. In *nature reviews materials* (Vol. 1, issue 12). Nature publishing group. doi:https://doi.org/10.1038/natrevmats.2016.71.

Li, J., & Mooney, D. J. (2016b). Designing hydrogels for controlled drug delivery. In *nature reviews materials* (Vol. 1, issue 12). Nature publishing group. doi:https://doi.org/10.1038/natrevmats.2016.71.

Lin, G., Chang, S., Kuo, C. H., Magda, J., & Solzbacher, F. (2009). Free swelling and confined smart hydrogels for applications in chemomechanical sensors for physiological monitoring. *Sensors and Actuators, B: Chemical, 136*(1), 186–195. https://doi.org/10.1016/j.snb.2008.11.001

Lin, Y. T., Will, T., Wickham, C., Boeree, P., Jack, D., & Keiser, M. (2023). Evolution of the RebiSmart® electromechanical autoinjector to improve usability in support of adherence to subcutaneous interferon Beta-1a therapy for people living with multiple sclerosis. *Patient Preference and Adherence, 17*, 1923–1933. https://doi.org/10.2147/PPA.S414151

Lugaresi, A., Colombo, B., Patti, F., Qiu, K., & Zhang, M. (2023). Global, regional, and national burden of multiple sclerosis from 1990 to 2019: Findings of global burden of disease study 2019. http://ghdx.healthdata.org/gbd-results-.

Lwata, M., & Carlson, S. S. (1993). A large chondroitin sulfate proteoglycan has the characteristics of a general extracellular matrix component of adult brain. In. *The Journal of Neuroscience, 13, Issue l*.

Mahad, D. H., Trapp, B. D., & Lassmann, H. (2015). Pathological mechanisms in progressive multiple sclerosis. *The Lancet Neurology, 14*(2), 183–193. https://doi.org/10.1016/S1474-4422(14)70256-X

Martini, M., Hegger, P. S., Schädel, N., Minsky, B. B., Kirchhof, M., Scholl, S., … Laschat, S. (2016). Charged triazole cross-linkers for hyaluronan-based hybrid hydrogels. *Materials, 9*(10). https://doi.org/10.3390/ma9100810

Metz, L. M., Li, D. K. B., Traboulsee, A. L., Duquette, P., Eliasziw, M., Cerchiaro, G., … Yong, V. W. (2017). Trial of minocycline in a clinically isolated syndrome of multiple sclerosis. *New England Journal of Medicine, 376*(22), 2122–2133. https://doi.org/10.1056/nejmoa1608889

Mihajlovic, M., Rikkers, M., Mihajlovic, M., Viola, M., Schuiringa, G., Ilochonwu, B. C., … Vermonden, T. (2022). Viscoelastic chondroitin sulfate and hyaluronic acid double-network hydrogels with reversible cross-links. *Biomacromolecules, 23*(3), 1350–1365. https://doi.org/10.1021/acs.biomac.1c01583

Miyazaki, T., Yomota, C., & Okada, S. (1995). *Interaction between sodium hyaluronate and tetracycline*.

Novoskol'tseva, O. A., Rogacheva, V. B., Zezin, A. B., Joosten, J., & Brackman, J. (2009). Formation and transformations of polyelectrolyte gel-ampholyte dendrimer-surfactant ternary complexes. *Polymer Science - Series A, 51*(6), 598–605. https://doi.org/10.1134/S0965545X09060030

Pang, T., Wang, J., Benicky, J., & Saavedra, J. M. (2012). Minocycline ameliorates LPS-induced inflammation in human monocytes by novel mechanisms including LOX-1, Nur77 and LITAF inhibition. *Biochimica et Biophysica Acta - General Subjects, 1820*(4), 503–510. https://doi.org/10.1016/j.bbagen.2012.01.011

Peppas, N. A., Bures, P., Leobandung, W., & Ichikawa, H. (2000). Hydrogels in pharmaceutical formulations. www.elsevier.com/locate/ejphabio.

Rehmann, M. S., Skeens, K. M., Kharkar, P. M., Ford, E. M., Maverakis, E., Lee, K. H., & Kloxin, A. M. (2017). Tuning and predicting mesh size and protein release from step growth hydrogels. *Biomacromolecules, 18*(10), 3131–3142. https://doi.org/10.1021/acs.biomac.7b00781

Richbourg, N. R., & Peppas, N. A. (2020). The swollen polymer network hypothesis: Quantitative models of hydrogel swelling, stiffness, and solute transport. In Progress in polymer science (Vol. Vol. 105). Elsevier Ltd. doi:https://doi.org/10.1016/j.progpolymsci.2020.101243.

Rosas-Durazo, A., Hernández, J., Lizardi, J., Higuera-Ciapara, I., Goycoolea, F. M., & Argüelles-Monal, W. (2011). Gelation processes in the non-stoichiometric polylectrolyte-surfactant complex between κ-carrageenan and dodecyltrimethylammonium chloride in KCl. *Soft Matter, 7*(5), 2103–2112. https://doi.org/10.1039/c0sm00663g

Russo, M., Calabrò, R. S., Naro, A., Sessa, E., Rifici, C., D'Aleo, G., … Bramanti, P. (2015). Sativex in the Management of Multiple Sclerosis-Related Spasticity: Role of the corticospinal modulation. *Neural Plasticity, 2015*. https://doi.org/10.1155/2015/656582

Samantray, S., Olubiyi, O. O., & Strodel, B. (2021). The influences of sulphation, salt type, and salt concentration on the structural heterogeneity of glycosaminoglycans. *International Journal of Molecular Sciences, 22*(21). https://doi.org/10.3390/ijms222111529

Servaty, R., Schiller, J., Binder, H., & Arnold, K. (2001). Hydration of polymeric components of cartilage-an infrared spectroscopic study on hyaluronic acid and chondroitin sulfate. In. *International Journal of Biological Macromolecules, 28*. www.elsevier.com/locate/ijbiomac.

Shamkani, F., Barzi, S. M., Badmasti, F., Chiani, M., & mirabzadeh, E., Zafari, M., & Shafiei, M.. (2023). Enhanced anti-biofilm activity of the minocycline-and-gallium-nitrate using niosome wrapping against Acinetobacter baumannii in C57/BL6 mouse pneumonia model. *International Immunopharmacology, 115*. https://doi.org/10.1016/j.intimp.2022.109551

Shimojo, A. A. M., Pires, A. M. B., Lichy, R., Rodrigues, A. A., & Santana, M. H. A. (2015). The crosslinking degree controls the mechanical, rheological, and swelling properties of hyaluronic acid microparticles. *Journal of Biomedical Materials Research - Part A, 103*(2), 730–737. https://doi.org/10.1002/jbm.a.35225

Singh, M., & Bachhawat, B. K. (1968). ISOLATION AND CHARACTERIZATION OF GLYCOSAMINOGLYCANS IN HUMAN BRAIN OF DIFFERENT AGE GROUPS. In. *Journal of Neurochemistry, 15* (Pergamon Press. Printed in Northern Ireland).

Soliman, G. M., Choi, A. O., Maysinger, D., & Winnik, F. M. (2010). Minocycline block copolymer micelles and their anti-inflammatory effects on microglia. *Macromolecular Bioscience, 10*(3), 278–288. https://doi.org/10.1002/mabi.200900259

Stojkov, G., Niyazov, Z., Picchioni, F., & Bose, R. K. (2021). Relationship between structure and rheology of hydrogels for various applications. In *gels* (Vol. 7, issue 4). MDPI. doi:https://doi.org/10.3390/gels7040255.

Sun, T. L., Kurokawa, T., Kuroda, S., Ihsan, A. Bin, Akasaki, T., Sato, K., Haque, M. A., Nakajima, T., & Gong, J. P. (2013). Physical hydrogels composed of polyampholytes demonstrate high toughness and viscoelasticity. Nature Materials, 12(10), 932–937. doi:https://doi.org/10.1038/nmat3713.

Sun, Y., Nan, D., Jin, H., & Qu, X. (2020). Recent advances of injectable hydrogels for drug delivery and tissue engineering applications. Polymer Testing, 81. doi:https://doi.org/10.1016/j.polymertesting.2019.106283.

Takeno, H., & Sato, C. (2016). Effects of molecular mass of polymer and composition on the compressive properties of hydrogels composed of Laponite and sodium polyacrylate. *Applied Clay Science, 123*, 141–147. https://doi.org/10.1016/j.clay.2016.01.030

Tan, M., Xu, Y., Gao, Z., Yuan, T., Liu, Q., Yang, R., Zhang, B., & Peng, L. (2022). Recent advances in intelligent wearable medical devices integrating biosensing and drug delivery. In Advanced materials (Vol. Vol. 34, Issue 27). John Wiley and Sons Inc. doi:https://doi.org/10.1002/adma.202108491.

Tanaka, K. (1978). Physicochemical properties of chondroitin sulfate. *In J. Biochem, 83*.

Tao, Y., Ai, L., Bai, H., & Liu, X. (2012). Synthesis of pH-responsive photocrosslinked hyaluronic acid-based hydrogels for drug delivery. *Journal of Polymer Science, Part A: Polymer Chemistry, 50*(17), 3507–3516. https://doi.org/10.1002/pola.26159

Thang, N. H., Chien, T. B., & Cuong, D. X. (2023). Polymer-based hydrogels applied in drug delivery: An overview. In *gels* (Vol. 9, issue 7). Multidisciplinary digital publishing institute (MDPI). doi:https://doi.org/10.3390/gels9070523.

Toropitsyn, E., Ščigalková, I., Pravda, M., Toropitsyna, J., & Velebný, V. (2023). Enzymatically cross-linked hyaluronic acid hydrogels as in situ forming carriers of platelet-rich plasma: Mechanical properties and bioactivity levels evaluation. *Journal of the Mechanical Behavior of Biomedical Materials, 143*. https://doi.org/10.1016/j.jmbbm.2023.105916

Toropitsyn, E., Ščigalková, I., Pravda, M., & Velebný, V. (2023). Injectable hyaluronic acid hydrogel containing platelet derivatives for synovial fluid Viscosupplementation and growth factors delivery. *Macromolecular Bioscience, 23*(4). https://doi.org/10.1002/mabi.202200516

Visser, L. A., Huls, S. P. I., Uyl-de Groot, C. A., de Bekker-Grob, E. W., & Redekop, W. K. (2021). An implantable device to treat multiple sclerosis: A discrete choice experiment on patient preferences in three European countries. *Journal of the Neurological Sciences, 428*. https://doi.org/10.1016/j.jns.2021.117587

Wajda, D. A., & Sosnoff, J. J. (2015). Cognitive-motor interference in multiple sclerosis: A systematic review of evidence, correlates, and consequences. In , *Vol. 2015*. *BioMed Research international*. Hindawi Publishing Corporation. https://doi.org/10.1155/2015/720856.

Wang, Z., Nong, J., Shultz, R. B., Zhang, Z., Tom, V. J., Ponnappan, R. K., & Zhong, Y. (2017). Local delivery of minocycline from metal ion-assisted self-assembled complexes promotes neuroprotection and functional recovery after spinal cord injury. *Biomaterials, 112*, 62–71. https://doi.org/10.1016/j.biomaterials.2016.10.002

Wu, L., Chen, W., Li, F., Morrow, B. R., Garcia-Godoy, F., & Hong, L. (2018). Sustained release of minocycline from minocycline-calcium-dextran sulfate complex microparticles for periodontitis treatment. *Journal of Pharmaceutical Sciences, 107*(12), 3134–3142. https://doi.org/10.1016/j.xphs.2018.08.023

Xue, Y., Chen, H., Xu, C., Yu, D., Xu, H., & Hu, Y. (2020). Synthesis of hyaluronic acid hydrogels by crosslinking the mixture of high-molecular-weight hyaluronic acid and low-molecular-weight hyaluronic acid with 1,4-butanediol diglycidyl ether. RSC Advances, 10(12), 7206–7213. doi:https://doi.org/10.1039/c9ra09271d.

Zhang, Z., Nix, C. A., Ercan, U. K., Gerstenhaber, J. A., Joshi, S. G., & Zhong, Y. (2014). Calcium binding-mediated sustained release of minocycline from hydrophilic multilayer coatings targeting infection and inflammation. *PLoS One, 9*(1). https://doi.org/10.1371/journal.pone.0084360